GStructural and optical properties of $Mg_xZn_{1-x}O$ thin films by chemical spray pyrolysis (CSP) technique

Receved : 17/8/2016 **Accepted :30/10/2016**

Abdulazeez O. Mousa[1] , Saleem H. Trier[2]
[1]Department of Physics, College of Science, University of Babylon, P.O. Box 4, Babylon, Iraq
[2]Department of Environment, College of Science, University of Al- Qadisiyah, Diwaniya, Iraq
E-mail address:[1]Azizliquid_2005@yahoo.com, [2]Salemhamza79@yahoo.com

Abstract

In this paper was prepared $Mg_xZn_{1-x}O$ films using a chemical spraying pyrolysis (CSP) technique, and different proportions volumetric of Mg-content (0,30, 50, 70, and 90)%, and deposited on the glass substrates at a temperature of (450)°C, were thickness fixed by fixing a number sprinkles and was thickness of all the films ranges between(80±5)nm, was used as a gas holder nitrogen. The crystal structure was examined using X-ray diffraction (XRD) technique. The results showed that all the films prepared polycrystalline, showing improvement in the crystal. Were studied topography of the surface of the films prepared using atomic force microscopy (AFM), and showed that the grain size of the ZnO nanostructure depends on the ratio of Mg-content of volumetric, where decreases the grain size with increasing Mg-content. As well as the increase in the proportion of Mg-content in the films lead to a decrease in surface roughness. As has been the study of the optical properties of the films prepared through the optical transmittance measurements in the spectral region (300-700) nm. The results of the transmittance ranging from (82-94)% when increase the Mg-content from(30 to 90)%. It also was measured absorbance and the reflectivity of all the films. Also were measured absorption coefficient for all the films were its value higher than $(10^4)cm^{-1}$. The optical constants such as refractive index, extinction coefficient and dielectric constant have been calculated for all preparing films.

Keywords: Chemical spray, MgZnO, structural and optical properties

Subject Classification: QC 170-197

1. Introduction

Zinc oxide (ZnO) crystallize preferentially in the stable hexagonal wurtzite structure at room temperature and normal atmospheric pressure. It has lattice parameters a= (0.325) nm,and c = (0.521) nm with a density of (5.606) g. cm^{-3}. The electronegativity values of and O^{-2} Zn^{+2} are (3.44) and (1.65) respectively, resulting in very strong ionic bonding between Zn^{+2} and O^{-2}. Its wurtzite structure is very simple to explain, where each O^{-2} ion is surrounded tetrahedral by four Zn^{+2} ions and vice versa, stacked alternatively along the c-axis. It is clear that this kind of tetrahedral arrangement of O^{-2} and Zn^{+2} in ZnO will form a noncentral symmetric structure composed of two interpenetrating hexagonally closed packed sub-lattices of Zn and O that are displaced with respect to each other by an amount of (0.375) along the hexagonal axis. This is responsible for the piezoelectricity observed in ZnO, and it also plays a an important role in crystalline growth, defect generation and etching [1]. (MgO) is a highly ionic crystal solid which crystallized into a rock salt structure, it has (FCC) Mg^{+} and O^{-} sublattice and low energy neutral (100) cleavage planes, viewed as an arrangement of hard sphere bound together by electrostatic forces. In an MgO unit cell (14) O ions are closed packed into a face-centered cubic structure, while (12) Mg ions are located at the center of the cube edges and one magnesium ion located at the cube center MgO is typical wide energy gap (7.8) eV semiconductor, represents an important class of functional metal oxides with a broad range of properties. The addition of impurities among the wide energy gap semiconductors often induces dramatic changes in their structural and optical properties. Furthermore, the bonding strength of Mg-O is stronger than that of Zn-O, therefore MgZnO is expected to have higher lattice stability than ZnO [2]. The aims of this paper to reveal specific properties of $Mg_xZn_{1-x}O$ thin films nanocrystalline materials. Initially the group of samples have been prepared by (CSP) technique at different work conditions on glass substrates. That supposed to result in the different structural and surface morphology properties of the nanostructures to be obtained, also the optical and photoluminescence properties.

2. The theoretical part

The many crystal phases available in transparent conductive oxides(TCOs), hexagonal structure is the dominant phase in ZnO material, hexagonal phase is characterized by determining the a-lattice constant and c-lattice constant from X-ray spectrum and by using the following formula [3]:

$$\frac{1}{d_{hkl}^2} = \frac{4}{3}\left(\frac{h^2+hk+k^2}{a^2}\right) + \frac{l^2}{c^2} \quad (1)$$

Where (hkl) are Miller indices ,the a-parameter is obtained from the plane (h00), while the plane (00l) is used to obtain c-parameter. In the case of cubic diamond phase such as crystalline silicon, the a-lattice constant can be obtained from [3]:

$$\frac{1}{d_{hkl}^2} = \left(\frac{h^2+k^2+l^2}{a^2}\right) \quad (2)$$

Where d_{hkl} interplanar spacing. Plays crystalline size of the material crystallized an important role in determining the properties of matter, and can be estimated from X-ray diffraction technique in a way full width at half maximum and called relationship Shearer [4].

$$D_s = \frac{0.9\ \lambda}{\beta\ cos(\theta)} \quad (3)$$

Where D_s crystalline size, β full width at half maximum, λ wavelength. Macrostrain can be calculated by angle X-ray diffraction (XRD) and full width at half maximum (FWHM) by the relationship:

$$S = \frac{\beta cos\theta}{4} \quad (4)$$

Where S macrostrain. After knowing the crystalline size by X-ray diffraction (XRD) technique the dislocation density(δ) can be calculated using the following relation:

$$\delta = \frac{1}{D_s^2} \quad (5)$$

Where δ dislocation density. As for number of crystalline layers N_ℓ which could be calculated due to the percolation theory, and it depends on the film thickness (t) as the relation [5]:

$$N_\ell = \frac{t}{D_s} \quad (6)$$

The intensity of the photon flux decreases exponentially with distance through the semiconductor according to the following equation [6].

$$I = I_o \exp(-\alpha t) \quad (7)$$

Where I_o, I are the incident and the transmitted photon intensity respectively and α is the absorption coefficient. The direct transition in general occurs between top of valence band and bottom of conduction band (vertical transition) at the same wave vector ($\Delta k=0$) for conservation of momentum. This transition is described by the following relation [7].

$$\alpha h\upsilon = B'\left(h\upsilon - E_g\right)^{1/2} \quad (8)$$

Where B' is inversely proportional to amorphusity, $h\upsilon$ is the photon energy, E_g is the energy gap. The refractive index value can be calculated from the formula [8].

$$n = \left(\frac{4R}{(R-1)^2} - k_o^2\right)^{1/2} - \frac{(R+1)}{(R-1)} \quad (9)$$

Where R is the reflectance, and can be expressed by the relation [9].

$$R = \frac{(n-1)^2 + k_o^2}{(n+1)^2 + k_o^2} \quad (10)$$

The extinction coefficient, which is related to the exponential decay of the wave as it passes through the medium, is defined as [8].

$$k_o = \frac{\alpha\lambda}{4\pi} \quad (11)$$

The real and imaginary part of dielectric constant can be calculated by using the following equation [7].

$$(n - ik)^2 = \varepsilon_r - i\varepsilon_i \quad (12)$$

Where

$$\varepsilon_r = n^2 - k_o^2 \quad (13)$$

and

$$\varepsilon_{i=2nk} \quad (14)$$

3. The experimental part

The nanostructures $Mg_xZn_{1-x}O$ thin films were prepared by (CSP) technique under ambient atmosphere on glass substrate, when the different Mg-contents (0,30,50,70,and 90)%, temperature (450)^oC, and under pressure nitrogen (4.5)bar. X-ray diffraction (XRD) is one of the most powerful techniques for qualitative and quantitative analysis of crystalline composites. This technique has long been used to determine the general structure of solids such as thin films, including crystalline size, lattice constants, interplanar spacing, orientation of crystals (single or polycrystalline),defects, etc. In this study XRD type Shimadzu, power diffraction system with Cu-Kα X-ray tube (λ =1.54) Á is used. The X-ray scans are performed between 2θ values of (20°-60°). The FESEM study carried out by (S-4300 of Hitachi, S-4700 FESEM in Islamic republic of Iran/ university of Tehran/ Razi foundation) scanning electron microscopy equipped with energy dispersive X-ray spectroscopy EDS. The operation principle of an AFM - type (Nanoscope III and dimension 3100) the consists of a cantilever and a sharp tip at end. The surface of the sample is scanned with the tip, whereas the distance between the sample surface and the tip is short enough, to allow the van der Waals forces between them which cause deflection of the cantilever. That the deflection follows Hooke's law and the spring constant of the cantilever is known, thus the amount of deflection and further, the topographical profile of the sample can be determined. Typically, the deflection is measured by using a laser spot reflected from the back surface of the cantilever into an array of photodiodes. The transmittance, absorbance, and reflectance optical of$Mg_xZn_{1-x}O$ thin films with different Mg-contents (x=0, 30,50,70,and90)% on silicon substrate, temperature(450)^oC, and under pressure nitrogen(4.5) bar, by using spectrophotometer (CARY100 CONC plus UV-Vis-NIR, Split-beam optics, dual detectors), for the wavelength range from (300-700) nm. The optical properties are calculated from these optical measurements.

4. Results and discussion

The results and discusses the effect of mixing, on the characterization structural and optical properties of the $Mg_xZn_{1-x}O$ films grown by (CSP),also the structural and optical measurements such as, X-ray diffraction (XRD) technique, surface morphological features by (AFM).The transmittance, absorbance, and reflectance optical by (UV-Vis).

4.1 X-ray diffraction (XRD):

Fig.1 shows the (XRD) profiles of $Mg_xZn_{1-x}O$ thin films deposited at a substrate temperature of(450)^oC for different Mg-contents (x=0,30,50,70,and 90)%. The presence of diffraction peaks indicates that the film is polycrystalline with a hexagonal wurtzite type crystal structure. It revealed that the film have

three diffraction peaks corresponding to (100), (002), and (101) directions of the hexagonal ZnO crystal structure which is corresponding to the positions 2θ = (31.65^o, $34,5^o$, and 36.31^o) respectively as shown in Table1. It can be concluded that the thin films deposited in these experimental conditions show strong c-axis (002) orientation growth. When mixing Mg-content ratios referred to previously, and when certain conditions arise, there are three phases, the first phase remains structure of the hexagonal wurtzite, but down the intensity of the diffraction peaks as shown in Fig.1b, the second phase turns into a mixture of MgO is incorporated with ZnO as shown in Fig.1c , the third phase turns into the cubic rock salt structure for the appearance of MgO diffraction peaks are clear as shown in Figs.(1d,and e). In the first case,(i.e. when the Mg-content ratio (30)%) do not show any peaks additional, while in the second case, (i.e. when the Mg-content (50)% we note the appearance of two peaks two additional with directions (111),(200) corresponding to the angles of diffraction ($36.87^o$and 42.85^o), respectively. While in the third case, (i.e. when the Mg-contents (70 and 90)%) we note to increase the intensity of new peaks and the weakness of ZnO peaks and then vanish these results are consistent with research [10]. By increasing Mg-content x=(90)%, we have a peak for (200) films which deals with the sign of cubic single phase that point out the deviation from wurtzite to rock-salt cubic structure in $Mg_xZn_{1-x}O$ /glass films. We obtain two phases at x=(70)% that showd the reflection of (002) wurtzite along with (200) cubic. The deviation in wurtzite structure increase due to the fact of the electronagativities where Mg lose electron easier that Zn (i.e. 1.65 for Zn is larger than that of the1.31 for Mg). The (002) and (200) peaks position are shifted to higher diffraction angles by increasing Mg-content, which demonstrate itself by the c-axis compression. This shows the onset of lattice strain in the films by the ionic radii of Mg^{+2} (0.057) nm and Zn^{+2} (0.060) nm difference. For several Mg-content (x)%, we figure out in Fig.2A the change in c-axis lattice constant and crystallite size of Mg_xZnO_{1-x}/glass films. We show that the size of crystallite decrease from (32.75 to 21.99) nm as well as the evaluated c-axis lattice constant decrease monotonically from (5.210 to 5.138) nm by increasing in Mg-contents from (x=0 to 70)% and (x=0 to 90)%,respectively indicating c-axis compression as shown in Fig.2B. The (a ,and c) lengths determined by XRD are plotted as a function of Mg-content in Fig. 2B. This figure the a-axis lengths increase when increasing Mg-contents from (x= 0 to 90)%, while the c-axis length decrease. It is thought that the decreasing of c-axis lattice constant comes from increasing the number of Mg^{+2} ions incorporated into the interstitial sites and is assumed also that the c-axis lattice constant decreases slightly due to the increase of the number of substitutional Mg^{+2} ions, because the radius of Zn^{+2} ions is a little greater than that of radius Mg^{+2} ion, the decrease of the number of Zn^{+2} ion in the Zn lattice sites will compress the lattice constant, which are in agreement with the reports [11]. Also, the FHWM inversely proportional to the grain size as shown in Fig.2C.Fig.2D explains the relationship between each of the microstrain and dislocation density versus Mg-content, when increasing the Mg-content increases crystalline defects and this is attributable to the grain size, where it is reduced to increase the Mg-content and thus increasing the crystalline defects. It remains to refer to the diffraction peaks with increase of Mg-content shifted toward larger angles. All parameters were calculated and included in the Table1. Through what has been mentioned we note best Mg-content ratio is (30)%.

4.2 Atomic force microscopy (AFM)

AFM technique is a useful method analysis of the surface topography of the thin films. Fig.3 shows 2-D and 3-D AFM images for the Mg_xZnO_{1-x}/glass thin films at temperature (450) ^oC, nitrogen pressure (4.5) bar, using different Mg-contents (x= 0, 30, 50, 70, and 90)% with scanning area (200×200)nm^2 that showed the variation of surface roughness with Mg-content in the layers. As can be noticed from this figures, the nanocrystalline $Mg_xZn_{1-x}O$ films has high degree of homogeneity and the small grains has uniform distribution on the glass substrate. Root mean square (RMS) values are (1.71,0.573, 1.04, 0.61, and 0.533) nm with Mg-contents (x= 0, 30, 50,70,and 90)% respectively. It is found from the

AFM studies that the average diameter of the films increases with increasing the Mg-content, while the total grain size decreases. Surface thickness, roughness average and root mean square are of the films decreases with increasing the Mg-content. This is in agreement with the research [12]. On the other hand, root mean square (RMS) roughness is defined as the standard deviation of the surface height profile from the average height, is the most commonly reported measurement of surface roughness. Average diameter, total grain No., surface thickness, roughness average and root mean square for $Mg_xZn_{1-x}O$/glass thin films are shown in the Table 2.

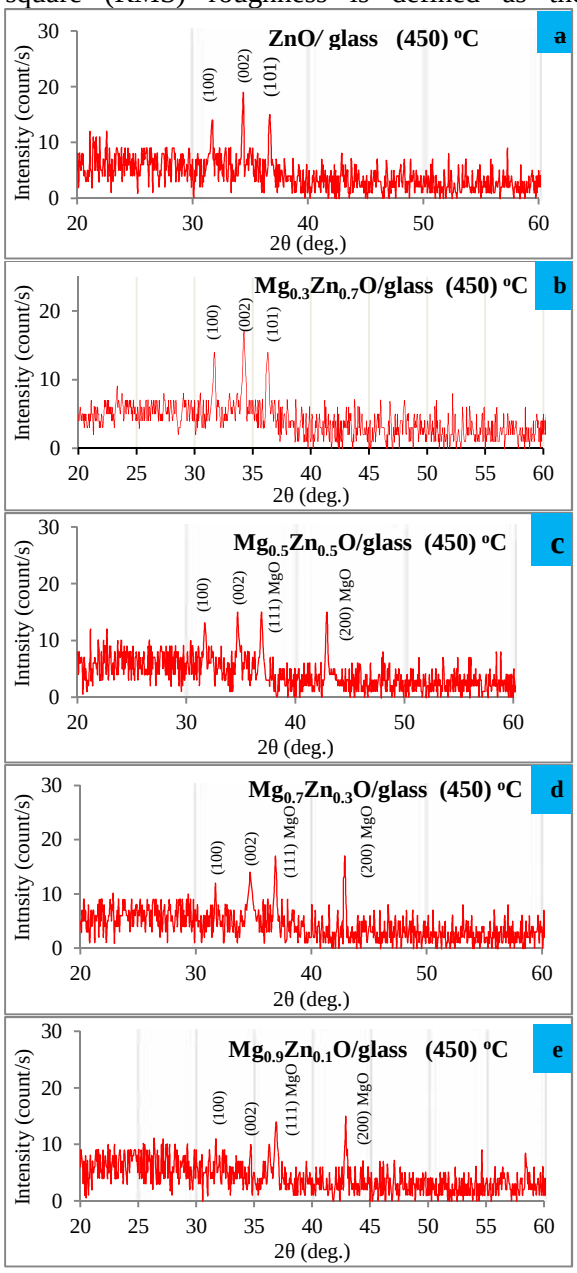

Fig.1: XRD patterns for $Mg_xZn_{1-x}O$/glass thin films with different Mg-contents (0,30,50,70,and 90)% and at temperature (450) °C

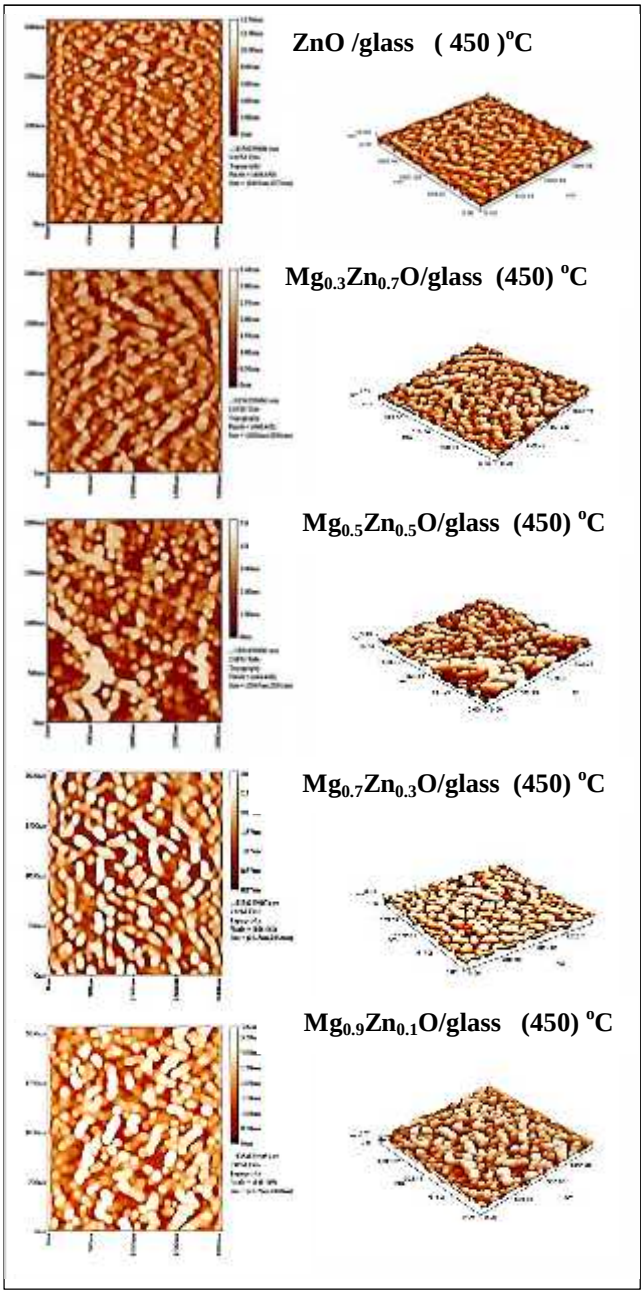

Fig.3: 2-D and 3-D AFM of $Mg_xZn_{1-x}O$ / glass with different Mg-content (0,30,50,70,and 90)% , and at substrate temperature (450)°C.

Table 1: The G_s , δ, S, and N_ℓ of layers data of (002),(200) orientations for $Mg_xZn_{1-x}O$/glass at different Mg-content, and substrate temperature (450) °C.

Sample	Investigated line(hkl)	2θ (deg.)	θ (deg.)	d(nm)	FWHM (β) (deg.)	Grain size G_s(nm)	δ×10^{15} (lin m^{-2})	S×10^{-3} (lin^{-2} m^{-4})	(N_ℓ)
ZnO	(100)	31.70	15.850	2.819	0.241	34.30	0.85	1.010	2.33
	(002)	34.38	17.190	2.605	0.352	23. 65	1.79	1.470	2.38
	(101)	36.70	18.350	2.446	0.208	40.29	0.62	0.854	1.99
$Mg_{0.3}Zn_{0.7}O$	(100)	31.65	15.825	2.823	0.281	29.37	1.16	1.180	2.72
	(002)	34.77	17.385	2.577	0.320	26.00	1.48	1.330	3.08
	(101)	36.35	18.175	2.468	0.244	34.30	0.85	1.010	2.33
$Mg_{0.5}Zn_{0.5}O$	(100)	31.64	15.82	2.824	0.235	31.5	1.01	0.986	2.54
	(002)	34.7	17.35	2.582	0.419	35.17	0.81	1.740	2.27
	(111)	36.85	18.425	2.436	0.473	17.70	3.19	1.960	4.52
	(200)	42.85	21.425	2.108	0.540	15.80	4.01	2.187	5.4
$Mg_{0.7}Zn_{03}O$	(100)	31.63	15.815	2.825	0.300	27.55	1.37	1.26	2.9
	(002)	34.75	17.375	2.578	0.392	21.25	2.21	1.632	3.76
	(111)	36.90	18.45	2.433	0.413	20.29	2.43	1.707	3.94
	(200)	42.80	21.40	2.110	0.452	18.88	2.80	1.834	4.24
$Mg_{0.9}Zn_{0.1}O$	(100)	31.72	15.86	2.818	0.138	59.74	0.28	0.577	1.34
	(002)	34.70	17.350	2.582	0.120	69.30	0.21	0.501	1.15
	(101)	36.25	18.125	2.475	0.388	21.55	2.15	1.608	3.71
	(111)	36.85	18.425	2.436	0.373	22.46	1.98	1.544	3.56
	(200)	42.87	21.435	2.107	0.448	19.10	2.74	1.817	4.19

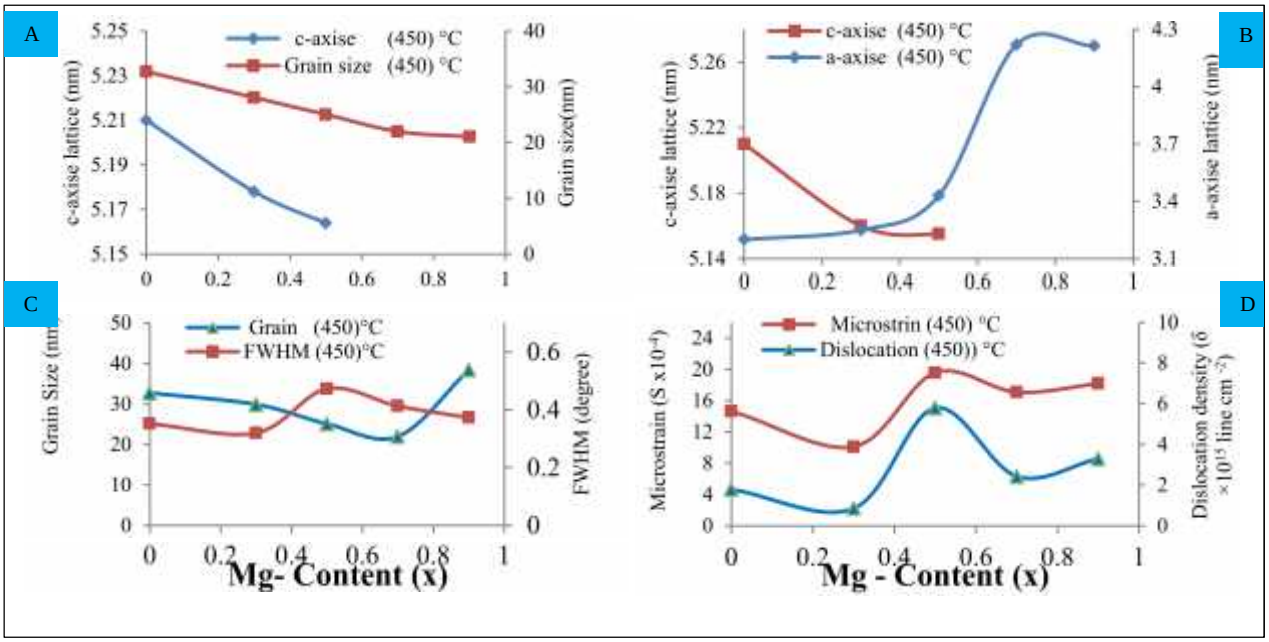

Fig.2: The variation of the lattice constants (a, and c), FWHM, G_S ,S, and δ versus different Mg-content for $Mg_xZn_{1-x}O$ /glass thin films at substrate temperature (450)°C

Table 2: Average diameter,total grain No., surface thickness, roughness average and root mean square for $Mg_xZn_{1-x}O$ /glass thin films at different Mg content (0,30,50,70, and 90)%, and temperature (450) ^oC.

Glass substrate			Ts =(450) ^oC , thickness = (80)nm		
Concentration (x)	Average diameter (nm)	Total grain No. (nm)	Surface thickness (nm)	Roughness average (nm)	Root mean square (nm)
ZnO (pure)	76.120	279	13.580	1.460	1.710
$Mg_{0.3}Zn_{0.7}O$	103.640	163	3.480	0.485	0.573
$Mg_{0.5}Zn_{0.5}O$	92.610	189	5.150	0.898	1.040
$Mg_{0.7}Zn_{0.3}O$	101.880	147	3.110	0.528	0.610
$Mg_{0.9}Zn_{0.1}O$	81.550	136	3.840	0.653	0.533

5. Optical properties

The optical properties of the $Mg_xZn_{1-x}O$ /glass thin films prepared by (CSP) technique under ambient atmosphere are measured by (UV-Vis) spectrophotometer at substrate temperature (450)°C in the range (300-700)nm. The nitrogen pressure is maintained at (4.5)bar various Mg-contents (x=0.,30,50,70,and 90)% with film average thickness (80±5)nm. The transmittance, absorbance and reflectance have been studied. Also the optical energy gap and optical constants have been determined.

5.1 Transmittance (T)

The transmittance spectra of the mixed $Mg_xZn_{1-x}O$ /glass films in the spectral range of (300-700) nm are compared as a function of Mg-content of (x)% as shown in Fig.4a. The average transmittance in the wavelength of visible region (430-700) nm varies between (76-82)%, when x=0, pure ZnO. Continue to increase with increasing concentrations of MgO in the films and up to (94)% when the concentration ratio (90)%. Displacement toward the shorter wavelength with increasing Mg-content clearly reflects the merger of Mg in the lattice of ZnO, indicating that the optical energy gap expanded with the addition of Mg regardless of crystallization, which is consistent with the report [13,14]. The increase in transmittance to increase the Mg-contents attributed to the increase in temperature, which leads to increased crystallization and thereby increase the transmittance. We show that the best transmittance of the mixed thin films was at x=(90)% , $Mg_{0.9}Zn_{0.1}O$/glass.

5.2 Absorbance (A)

We measure the spectral absorption of the mixed $Mg_xZn_{1-x}O$/glass films in the visible region are compared as a function of Mg-content of(x)% as shown in Fig.4b. The average absorbance for the visible region wavelength varies between (0.119-0.088) % for x=0 we have pure ZnO while at x = (30)% $Mg_{0.3}Zn_{0.7}O$ the absorbance varies between (0.351-0.161)%.Concentration ratio has been characterized (30)% as she was with high absorbency compared to other ratios. This interesting feature may be related to the solubility of Mg-atoms in the ZnO structure and may point to an increase in the localized impurity levels in the energy gap of ZnO as the concentration of Mg is raised.

5.3 Reflectance (R)

Increasing the reflectivity of the $Mg_xZn_{1-x}O$ / glass films compared with pure ZnO films, and tend to saturation at high wavelengths as shown in Fig.4c. Vary the reflectivity increases and decreases when the temperature (450) ^oC depending on the preparation of thin films and the deposition technique.

5.4 Absorption coefficient (α)

Fig.4d shows the absorption coefficient (α) of the $Mg_xZn_{1-x}O$ thin films with different Mg-contents determined from absorbance measurements. The (α) of $Mg_xZn_{1-x}O$ thin films increased sharply in the region of UV-Vis, and then decreased sharply in the visible region because it is inversely proportional to the transmittance. The (α) is decreasing with the increase of Mg-content, its value is larger than (10^4) cm^{-1}. This can be related with decrease in grain size and it may be attributed to the light scattering effect for its low surface roughness.

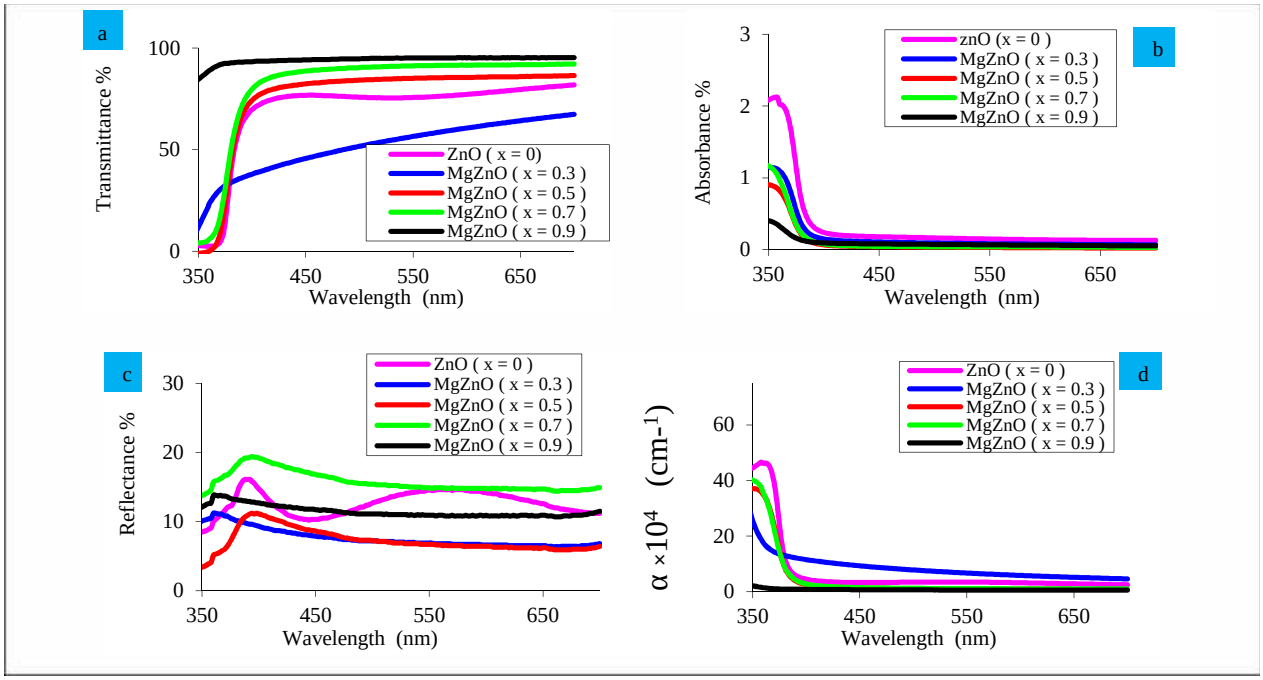

Fig.4: T, A, R, and α as a function of wavelength for $Mg_xZn_{1-x}O$ /glass thin films prepared in different Mg-contents (0 ,30,50 ,70,and 90)%, at (450) ^oC.

5.5 Optical energy gap (E_g)

The optical energy gap (E_g) of the $Mg_xZn_{1-x}O$ /glass thin films was estimated from the transmission or absorption spectra and the optical (α) near the absorption edge for direct transitions. The characteristics of $(\alpha h\upsilon)^2$ versus photon energy (hυ) were plotted for evaluating the (E_g) of the $Mg_xZn_{1-x}O$ thin films, and extrapolating the linear portion near the onset of absorption edge to the energy axis as shown in Fig.5. values (E_g) of $Mg_xZn_{1-x}O$ thin films are (3.21,30.3,3.22,3.21,and 3.40) corresponding to theMg-content(x=0,30,50,70,and90)% respectively.

5.6 Refractive index (n)

The (n) of the $Mg_xZn_{1-x}O$ thin films, as shown in Fig.6a the (n) of the films are influenced by the Mg-content. The (n) increase with the Mg-content increases in the range of(3.13-3.23) respectively.(n) decrease as the wavelength increases, the decreases in grain size with the increasing of refractive index is observed. The increase of (n) may be due to increase the crystalline defects ,the decrease in grain size and the increase in microstrain, a clear indication of the refractive index increase with Mg-content increase.

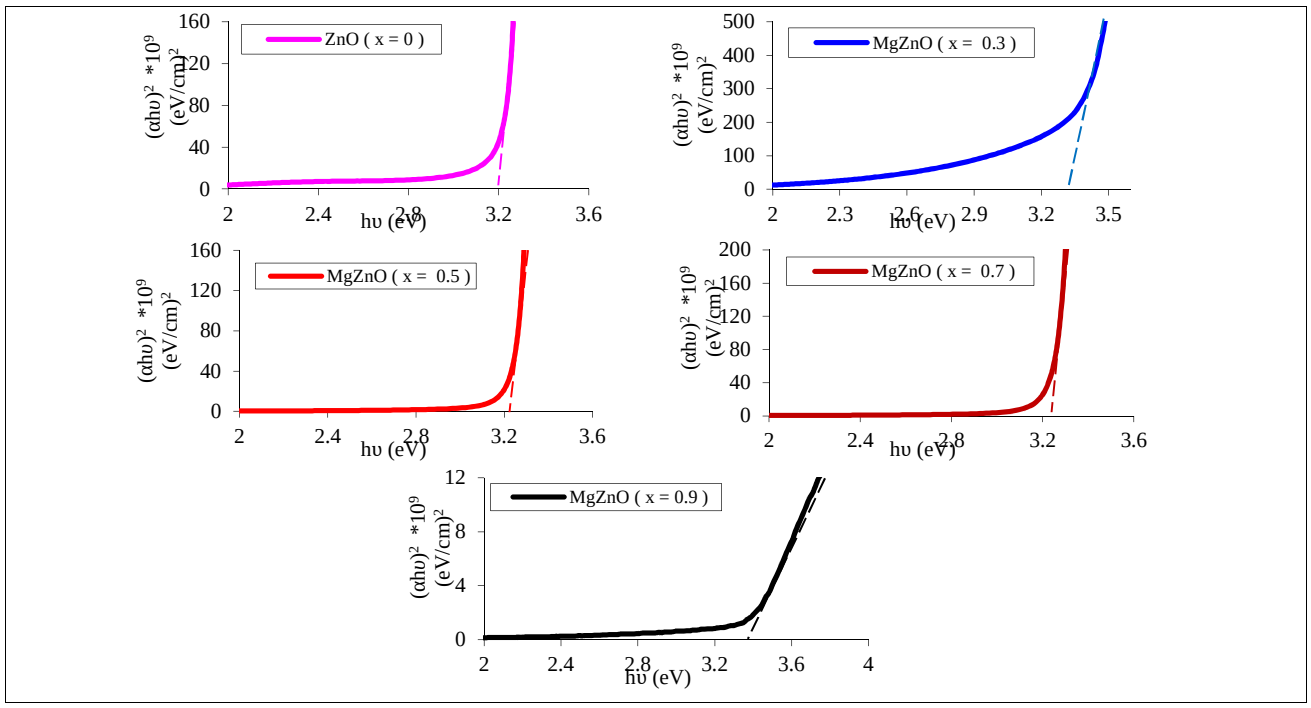

Fig.5: $(\sim h\upsilon)^2$ versus photon energy for $Mg_xZn_{1-x}O$ /glass thin films in different Mg-contents (0 ,30 ,50 ,70, and 90)% at (450) ^oC

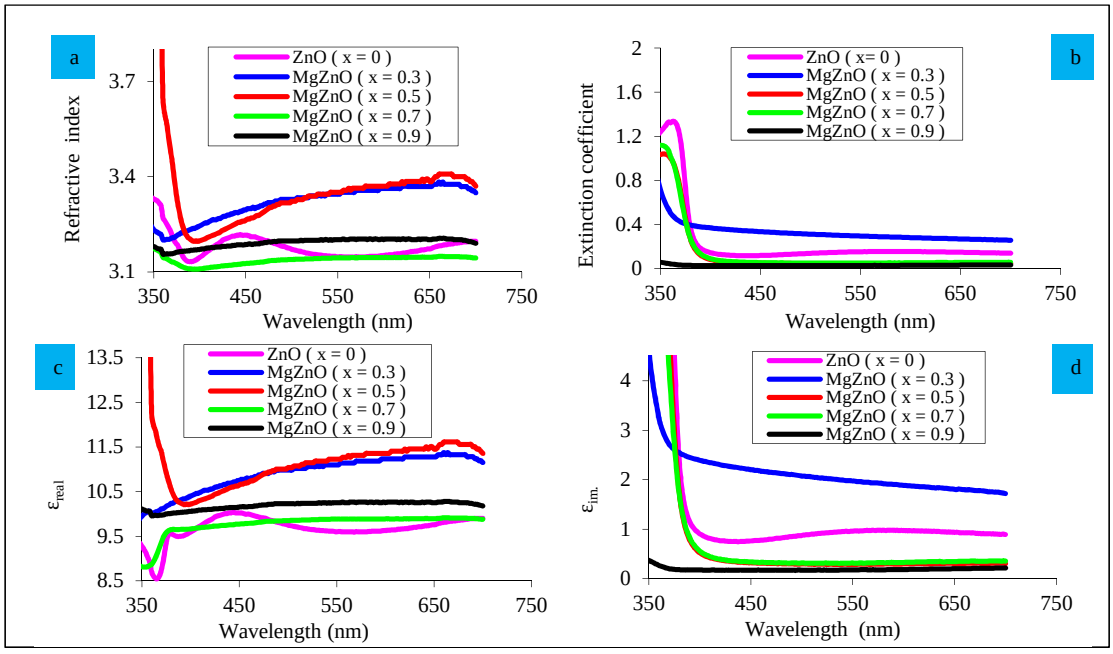

Fig.6: Variation of n, k_o , $£_r$, and $£_i$ as a function of wavelength for $Mg_xZn_{1-x}O$ /glass films in different Mg-contents (0,30,50,70, and 90)%, at (450) ^oC

5.7 Extinction coefficient (k_o)

Fig.6b, shows the extinction coefficient (k_o) as a function of wavelength (λ) for pure ZnO and $Mg_xZn_{1-x}O$/glass. It's clear from the figure that the (k_o) has the same behavior (α), but increase of substrate temperature leads to decreases the defects or the tails within the energy gap so decrease the (k_o) values in the pure ZnO. Also shows the effect of concentration of MgO on the (k_o) values.In general, we note that the maximum value of (k_o) when the absorption edge and then decrease sharply when the visible region of wavelengths, and when increasing the Mg-content shifted absorption edge toward shorter wavelengths (i.e., high-energy).

5.8 Real and imaginary part of dielectric constant (ε_r), (ε_i)

An absorbing medium is characterized by a complex dielectric constant. The real and imaginary part of dielectric constant of the $Mg_xZn_{1-x}O$/glass thin films by chemical spray pyrolysis (CSP) technique, as shown in Figs.(6c,and d). The variation of (ε_r), (ε_i) with wavelength for pure ZnO and $Mg_xZn_{1-x}O$ thin films. The obtained results show that the values of real and imaginary part of dielectric constant are decreased with increasing of wavelength for $Mg_xZn_{1-x}O$ thin films, thus the complex dielectric constant are reduce to increase the Mg-content in the films.

6. Conclusions

Through the study was concluded following points:

1- The addition of Mg to the films increases the her strength to withstand high temperatures and little of expansion.
2- The films deposited from Mg mixed ZnO thin films at nitrogen pressure of (4.5) bar, and substrate temperature (450)^{o}C are good candidates for structural, morphology and optical properties.
3- The structural of the ZnO films are found what dependent on the films mixed , (i.e. an increase of the mixture concentration into the film). The results of (XRD) shows that all thin films (pure and mixed) exhibit polycrystalline nature, and has the hexagonal wurtzite structure with preferential orientation in the (002) plane, when the Mg-content ratio (30)%, It turns into a cubic rock salt structure when increasing the Mg-content ratios higher than (50)% with preferential orientation in the (200) plane.
4- The AFM results show the slow growth of nanocrystallite sizes for the as grown films. The root mean square (RMS) is decreasing when increase the Mg-content up to x= (90)%. XRD, and AFM analysis shows that the prepared films are nanocrystalline thin films with estimated comparable grain sizes.
5- The optical properties of $Mg_xZn_{1-x}O$ thin films show that the films have direct transition. The average transmittance for all the films is over (90)% in the wavelength range (300-700) nm and the transmittance invisible region increases with the increase Mg-content. The optical energy gap is dependent on the Mg-content, increasing in the mixing ratio for Mg cause an increase in the optical energy gap value, also the values of refractive index (n) of $Mg_xZn_{1-x}O$ films lie in the range of (3.13-3.23). This means that the film suitable for photodetectors applications.

7. References

[1] Robertson, J., and Falabretti, B., "Electronic structure of transparent conducting oxides",in Handbook of transparent conductors, Springer Science +Business Media, New York, pp. (27-50), (2010).

[2] Gao, J., Zhao, G.J., Liang, X.X. and Song, T.L.," First-principles study of structural properties of $Mg_xZn_{1-x}O$ ternary alloys", Journal of Physics Conference Series, Vol.574 , pp.(1-6) ,(2015).

[3] Saeed, N. M., "Structural and optical properties of ZnS thin films prepared by spray pyrolysis technique", Journal of Al-Nahrain University, Vol.14 , pp.(86-92), (2011).

[4] Sengupta, J., Ahmed, A. and Labar, R. "Structural and optical properties of post annealed Mg doped ZnO thin films deposited by the sol-gel method",

Materials Letters, Vol.109 , pp. (265-268), (2013).

[5] Kazmerski, L.L. "Polycrystalline and amorphous thin films and device",6th edition, Lawrence Academic Press, New York, (1980).

[6] Elliot ,R. J., and Gibson, A.F, "An introduction to solid state physics and its application", 1st edition, Macmillan Inc., (1974).

[7] Kazmerski, L.L., "Polycrystalline and amorphous thin films and device",6th edition, Lawrence Academic Press, New York, (1980).

[8] Moss, T. S., "Optical properties of semiconductors", London butterworths scientific Puplications, New York , Academic Press (1959).

[9] Grenier,R., "Semiconductors device and electronic energy series", Mc Graw-Hill, Book Co. Inc. (1961).

[10] Agrawal, A., Dar, T., Dar, A. and Sen, P., "Structural and optical studies of Mg doped ZnO thin films", Journal of Nano- and Electronic Physics Vol.5, pp.(1-3), (2013).

[11] Kim, M. S., Noh, K. T., Yim, K. G., Nam, S. G., Lee, D.-Y., Kim, J. S., Kim, J. S. and Leem, J.-Y.,"Composition dependence on structural and optical properties of $Mg_xZn_{1-x}O$ thin films prepared by Sol-Gel method", Bull. Korean Chem.Soc.,Vol.32,p.(3453- 3458), (2011).

[12] Tsay, C.-Y., Wang ,M.-C. and Chiang, S.-C.,"Effects of Mg additions on microstructure and optical properties of Sol-Gel derived ZnO thin films", Materials transactions, Vol.49, pp.(1186 - 1191), (2008).

[13] Ji, L. W., Lin, C. M. , Fang, T. H., Chu, T. T. , Jiang, H., Shi, W. S., Wua, C. Z., Chang, T. L., Meen T. H. and Zhong, J. Applied Surface Science, Vol.256, p.2138, (2010).

[14] Özgür, Ü., Alivov, Y. I., Teke,C. A., Reshchikov, M. A., Doğan, S., Avrutin, V., Cho, S.-J. and Morkocd, H., "A comprehensive review of ZnO materials and devices", Applied Physics Reviews, Vol.98, pp.(1-301) , (2005).

* دراسة بعض الخصائص الفيزيائية لأغشية Mg_xZnO_{1-x} باستخدام تقنية الرش الكيميائي الحراري

تاريخ الاستلام 2016/8/17 تاريخ القبول 2016/10/30

عبد العزيز عبيد موسى [1] ،سليم حمزة طرير جبر [2]
[1]قسم الفيزياء، كلية العلوم ، جامعة بابل، صندوق بريد 4 ، بابل، العراق
[2]قسم البيئة ، كلية العلوم ، جامعة القاسمية ، ديوانية ، العراق
E-mail address: [1]Azizliquid_2005@yahoo.com, [2]Salemhamza79@yahoo.com

الخلاصة
في هذا البحث تم تحضير أغشية $Mg_xZn_{1-x}O$ باستخدام تقنية الرش الكيميائي الحراري وبنسب حجمية مختلفة من محتوى المغنيسيوم (0، 30،50 ، 70 و 90) % والمرسبة على قواعد زجاجية عند درجة حرارة (450) درجة مئوية وتم تثبيت السمك من خلال تثبيت عدد الرشات وكان سمك جميع الاغشية يتراوح بين (80±5) نانومتر وقد تم استخدم غاز النيتروجين. و تم تشخيص التركيب البلوري للأغشية بتقنية حيود الأشعة السينية (XRD) و أوضحت النتائج إن جميع الأغشية المحضرة كانت متعددة التبلور وأظهرت تحسن البنية البلورية. و درست طبوغرافية السطح للأغشية المحضرة باستخدام مجهر القوى الذرية (AFM). وان الحجم الحبيبي النانوي لأوكسيد الزنك ZnO يعتمد على نسبة محتوى المغنيسيوم الحجمية، حيث ينخفض الحجم الحبيبي بزيادة محتوى المغنيسيوم. كذلك إن زيادة نسبة محتوى المغنيسيوم في الاغشية تؤدي إلى تقصان خشونة السطح. و تمت دراسة الخصائص البصرية للأغشية المحضرة من خلال قياسات الفاذية البصرية في المنطقة الطيفية (300 – 700) نانومتر. وكانت نتائج الفاذية تتراوح من (82- 94)% عند زيادة محتوى المغنيسيوم من (30– 90)%. و تم قياس الامتصاصية والانعكاسية لجميع الاغشية. بالإضافة الى ذلك تم قياس معامل الامتصاص لجميع الاغشية وكانت قيمته أعلى من (10^4) cm^{-1}. و تم حساب الثوابت البصرية كمعامل الانكسار ومعامل الخمود وثابت العزل الحقيقي والخيالي لجميع الأغشية المحضرة.

الكلمات المفتاحية: الرش الكيميائي، MgZnO، الخصائص التركيبية والبصرية
* البحث مستل من اطروحة دكتوراه للباحث الثاني.

* the research is a part of an Ph.D. dissertation in the case of the second researcher.